

# *Hedychium coronarium* extract arrests cell cycle progression, induces apoptosis, and impairs migration and invasion in HeLa cervical cancer cells

Asit Ray<sup>1,2</sup>  
Sudipta Jena<sup>2</sup>  
Biswabhusan Dash<sup>2</sup>  
Ambika Sahoo<sup>2</sup>  
Basudeba Kar<sup>2</sup>  
Jeetendranath Patnaik<sup>3</sup>  
Pratap Chandra Panda<sup>4</sup>  
Sanghamitra Nayak<sup>2</sup>  
Namita Mahapatra<sup>1</sup>

<sup>1</sup>Regional Medical Research Centre (Indian Council of Medical Research), Chandrasekharpur, Bhubaneswar 751023, Odisha, India; <sup>2</sup>Centre for Biotechnology, School of Pharmaceutical Sciences, Siksha O Anusandhan University, Kalinganagar, Ghatikia, Bhubaneswar 751003, Odisha, India; <sup>3</sup>Department of Botany, Sri Krushna Chandra Gajapati College, Paralakhemundi 761200, Odisha, India; <sup>4</sup>Taxonomy and Conservation Division, Regional Plant Resource Centre, Nayapalli, Bhubaneswar 751015, Odisha, India

Correspondence: Sanghamitra Nayak  
Centre for Biotechnology, School of  
Pharmaceutical Sciences, Siksha O  
Anusandhan University, Kalinganagar,  
Ghatikia, Bhubaneswar 751003, Odisha,  
India  
Tel +91 943 706 1976  
Email sanghamitran24@gmail.com

**Background:** *Hedychium coronarium* Koen. (Zingiberaceae) is traditionally used as medicine in countries such as India, China, and Vietnam for treatment of various ailments including cancer. However, in spite of its implied significance in cancer treatment regimes, there are no reports so far involving the anticancerous attributes of *H. coronarium* ethanol extract (HCEE) on cancer cells and a more comprehensive study on its mechanism is still lacking.

**Materials and methods:** The cytotoxicity of HCEE was evaluated by MTT and clonogenic survival assay. Annexin V/propidium iodide (PI), Hoechst 33342 staining, and TUNEL assay were performed to detect apoptosis. Cell cycle analysis was performed using PI staining. JC-1 and 2',7'-dichlorodihydrofluorescein diacetate assay were used to check the levels of MMP and ROS, respectively. Western blot analysis was carried out to measure the expression levels of proteins. Migration and invasion activity were assessed by wound healing and Transwell membrane assay, respectively.

**Results:** Antiproliferative effect of HCEE was investigated in various cancerous and normal cell lines. Among these, HCEE significantly inhibited the survival of HeLa cells without affecting the viability of normal human umbilical vein endothelial cells. Annexin V/PI, Hoechst staining, and TUNEL assay showed HCEE induced apoptosis in HeLa cells in a dose-dependent manner. HCEE promoted cell cycle arrest at G1 phase in HeLa cells by upregulating the levels of p53 and p21 and downregulating the levels of cyclin D1, CDK-4, and CDK-6. Moreover, HCEE treatment upregulated the expression of Bax and downregulated the expression of Bcl-2. Additionally, HCEE activated the caspase cascade by increasing the activities of caspase-9, caspase-8, and caspase-3. The expression levels of Fas ligand and Fas were also upregulated. Further, HCEE inhibited the migratory potential of HeLa cells by downregulating MMP-2 and MMP-9 expression levels.

**Conclusion:** Our results indicate *H. coronarium* exerts antiproliferative and apoptotic effects against HeLa cells, and therefore may be used for treatment against cervical cancer.

**Keywords:** apoptosis, cervical cancer, cytotoxicity, *Hedychium coronarium* extract, HeLa cell line

## Background

Cancer is a group of diseases involving abnormal growth of cells with the ability to invade different parts of the body.<sup>1</sup> According to the WHO estimates, cancer ranks among the most common leading causes of death with nearly 14 million new cases and 8.8 million deaths worldwide in the year 2012. Cervical cancer represents the third

leading cause of cancer death in females in the developing countries.<sup>2</sup> India accounts for nearly one-third of cervical cancer deaths worldwide, with ~132,000 new cases and 74,000 deaths reported each year.<sup>3</sup> The current screening methods to detect cervical cancer include cytological-based Pap smears and human papillomavirus (HPV) lesions detected through HPV testing.<sup>4</sup> However, in low- and middle-income countries, cytology-based screenings and HPV tests have not been effective due to low resources and lack of infrastructure.<sup>5</sup> Even though chemotherapy is used for the effective treatment of cancer, it suffers from severe side effects.<sup>6</sup>

The increased mortality rates in cancer patients have led researchers to search for potential plant-based natural products that can be used as alternative cancer therapeutic agents.<sup>7</sup> Several plant-derived phytochemicals are being used as potential drugs to kill abnormally growing cancerous cells.<sup>8–10</sup> These compounds are considered effective as they are safe, inexpensive, and have no side effects.<sup>11</sup> Clinical studies have shown that herbal drugs exert anticancer effects by inducing apoptosis, activating DNA repair systems, arresting cell cycle, and inhibiting angiogenesis.<sup>12–14</sup>

*Hedychium coronarium* (Zingiberaceae) is distributed in various parts of the world including India, China, Brazil, and South Eastern Asia.<sup>15</sup> Rhizomes of *H. coronarium* are used as a febrifuge, tonic, excitant, and antirheumatic in traditional system of Indian medicine.<sup>16</sup> The decoction of the stem is gargled for throat infection.<sup>17</sup> Several pharmacological and biological activities, such as anti-inflammatory, antibacterial, antifungal, and antioxidant activities, have been reported for *H. coronarium*.<sup>18–20</sup> *H. coronarium* is known for its potential cancer chemoprevention activity attributed to the presence of labdane diterpenes.<sup>21</sup> Several investigations have shown that labdane diterpenes isolated from *H. coronarium* extract display antiproliferative properties against several cancer cell lines in vitro.<sup>22–24</sup> However, no reports have shown the anticancer effect of *H. coronarium* extract on different cancerous cell lines. Moreover, the molecular mechanism of action through which *H. coronarium* extract interferes with the growth and progression of the tumor is hardly known. Therefore, the present research was aimed to elucidate the cytotoxic effect of *H. coronarium* extracts on various cancerous (A549, HeLa, PANC-1, LnCaP, and Jurkat) and normal (human umbilical vein endothelial cell [HUVEC]) cell lines. Further, the relationship of the antiproliferative effects with probable apoptosis, cell cycle arrest, migration, and invasion was studied in HeLa cells. Additional investigation about the expression of different proteins in the signal transduction

pathways of *H. coronarium* ethanol extract (HCEE)-induced apoptosis in HeLa cells was also carried out.

## Materials and methods

### Plant material and sample preparation

Rhizomes of *H. coronarium* in flowering stage were collected from Phulbani, Odisha, India (latitude N 19° 56' 31.3", longitude E 83° 39' 22.3"). The plant was taxonomically authenticated by the principal scientist, Dr PC Panda, Taxonomy and Conservation Division, Regional Plant Resource Center, Bhubaneswar, India, and a voucher specimen (RPRC/2017/9742) was submitted at the herbarium of the same institute. The rhizomes were washed, shade dried, powdered, and extracted in 70% ethanol using Soxhlet apparatus for 8 hours. The filtrates were concentrated under vacuum and reduced pressure (yield: 7.14%) using Rotary evaporator (Buchi, Labortechnik AG, Switzerland) and stored at -20°C until they were used. Then the extract was dissolved in dimethyl sulfoxide (DMSO) for preparation of various concentrations for cytotoxicity and other assays.

### Chemical and reagents

Acetonitrile, ethanol, water, paraformaldehyde, and DMSO were obtained from Merck (Darmstadt, Germany). Roswell Park Memorial Institute-1640, BSA, trypsin, streptomycin, DMEM, and penicillin were purchased from Himedia Chemicals Ltd (Mumbai, India). MTT reagent, 2',7'-dichlorodihydrofluorescein diacetate (DCFH-DA) reagent, JC-1 dye, Hoechst 33242, propidium iodide (PI), RNase A, crystal violet, methylene blue, Coomassie Brilliant Blue R-250, *N*-acetyl-L-cysteine (NAC), SDS, Triton-X 100, Tris-base, glycine, acrylamide, bisacrylamide, ammonium persulfate, tetramethylethylenediamine, Tween-20, biconchonic acid reagent, and 2-mercaptoethanol were purchased from Sigma-Aldrich. All antibodies were procured from Abcam (Cambridge, MA, USA). Annexin V-fluorescein isothiocyanate (FITC) apoptosis kit and APO Direct kit were obtained from BD Biosciences (San Jose, CA, USA). Caspase-3 substrate (Ac-DEVD-AMC), caspase-8 substrate (Ac-IETD-AMC), and caspase-9 substrate (Ac-LEHD-AMC) were obtained from Cayman Chemicals. Polyvinylidene difluoride membrane was purchased from Thermo Fisher Scientific (Waltham, MA, USA). Matrigel invasion chambers with 8 µm pore size inserts were obtained from BD Biosciences. The reference standards used, that is, coronarin-D (purity >99%) and coronarin-D methyl ether (purity >99%), were purchased from Wuhan ChemFaces Biochemical Co., Ltd (Wuhan, China).

## HPLC analysis

Rhizome extract was characterized using HPLC on a Waters 1525 binary HPLC pump (Milford, MA, USA) equipped with a Waters 2489 ultraviolet–visible detector. The column used was C<sub>18</sub> RP column Xbridge (5 μm particle size, 250×4.6 mm). The reference standards used were coronarin-D and coronarin-D methyl ether. The mobile phase consisted of a mixture of water (35%) and acetonitrile (75%), which was applied isocratically for 15 minutes. Both rhizome extract and reference standards were dissolved in HPLC-grade ethanol. Extract was filtered with 0.20 μm filter paper (Pall Lifesciences) before injection. A volume of 20 μL was injected with a flow rate of 1 mL/min. The chromatogram was detected at a wavelength of 254 nm.

## Calibration curves

Calibration curves were prepared with dilutions of 0.1, 0.2, 0.4, 0.8, and 1.6 mg/mL of the reference standards in ethanol. Calibration curves were prepared based on the average peak areas of each chromatogram. The calibration curve showed  $R^2=0.99$  for coronarin-D ( $Y=1.14+007 X+3.09 e+005$ ) and  $R^2=0.98$  for coronarin-D methyl ether ( $Y=7.82 e+007 X+9.98 e+005$ ).

## Cell culture

A549, HeLa, PANC-1, LnCaP, Jurkat, and HUVEC were procured from the cell repository, National Center for Cell Science (Pune, India). LnCaP and Jurkat cells were cultured in Roswell Park Memorial Institute-1640 medium. HUVECs were cultured in M199 supplemented with 10% FBS and endothelial cell growth supplement (Himedia Chemicals Ltd). A549, HeLa, and PANC-1 were maintained in DMEM supplemented with 10% FBS and with 1% penicillin–streptomycin. Stock solutions of the HCEE were dissolved in DMSO before they were diluted to working concentration in the medium, while untreated cell was used as a negative control. All the cells were incubated in a CO<sub>2</sub> incubator with 5% CO<sub>2</sub> at 37°C.

## Cytotoxicity assay

The cytotoxicity of *H. coronarium* extract was measured using MTT cell survival assay as previously described.<sup>25</sup> Briefly, cells at a seeding density of 1×10<sup>5</sup> cells/well were seeded into 96-well plates. Cells were then exposed to different concentrations (1, 10, 20, 40, 80, 160, and 320 μg/mL) of HCEE for 24 hours. The negative control included DMSO (0.1%). Following the treatment period, 20 μL of MTT reagent (5 mg/mL) was mixed in each well and kept for

4 hours at 37°C. After 4 hours, the medium was discarded, and 200 μL of DMSO was added and the plates were gently shaken. The absorbance of purple-colored formazan was recorded at 570 nm by an ELISA plate reader (BMG Labtech, Ortenberg, Germany). Camptothecin (0–10 μg/mL) was taken as a positive control. Each measurement was performed in triplicate. The percentage of cell viability (%) was measured from background-corrected absorbance as follows:

$$\text{Cell viability (\%)} = \left( \frac{\text{Absorbance of treated cells}}{\text{Absorbance of control cells}} \right) \times 100$$

## Clonogenic survival assay

Clonogenic assay was performed according to the previously established method.<sup>26</sup> Briefly, HeLa cells at a seeding density of 1×10<sup>5</sup> cells/well were plated onto six-well plates and incubated overnight. After incubation, cells were treated with 20 and 40 μg/mL concentration of HCEE and control (0.1% DMSO) and incubated for another 2 days. The cells were allowed to grow for another 7 days, followed by staining with 0.5% methylene blue and fixation in 50% methanol. The experiments were repeated three times, and colonies with >50% cells were counted. At the end, the results were expressed as the survival fraction, where

$$\text{Survival fraction} = \left( \frac{\text{Number of colonies formed after treatment}}{\text{Number of cell seeded}} \right) \times \text{PE}$$

$$\text{Plating efficiency (PE)} = \left( \frac{\text{Number of colonies formed}}{\text{Number of cell seeded}} \right) \times 100\%$$

## Hoechst 33342 staining

The morphological changes of HeLa cells were observed using Hoechst 33342 fluorescent stain as previously described.<sup>27</sup> The cells were cultured on six-well plates at a concentration of 3×10<sup>5</sup> cells/well and treated with various concentration of HCEE (0, 20, and 40 μg/mL) for 24 hours. After incubation, the cells were washed three times with PBS followed by staining with Hoechst 33342 for another 30 minutes at 37°C in dark. The nuclear morphology of Hoechst 33342-stained HeLa cells was examined under the fluorescence microscope (Nikon E 600; Nikon Corporation, Tokyo, Japan).

## Annexin V/PI apoptosis staining

Annexin V-FITC apoptosis kit (BD Biosciences) manual instructions were followed to measure the proportion of apoptotic HeLa cells. The cells were cultured in a six-well plate at a seeding density of  $1 \times 10^6$  cell/mL and incubated with various (0, 20, and 40  $\mu\text{g/mL}$ ) concentrations of HCEE at  $37^\circ\text{C}$ . The collected cells were washed with PBS twice and resuspended in 1X Annexin V binding buffer. Then, 100  $\mu\text{L}$  of cells was added to 5  $\mu\text{L}$  of Annexin V-FITC and 5  $\mu\text{L}$  of PI in a tube, followed by incubation at room temperature for 15 minutes. Then 400  $\mu\text{L}$  of 1X binding buffer was added to each tube and vortexed gently and subjected to flow cytometry within 1 hour. Final fluorescence of Annexin V-FITC was obtained in 10,000 events on BD FACSCANTO II flow cytometer (BD Biosciences).

## TUNEL assay

The apoptosis of HeLa cells was analyzed by TUNEL assay following the previously described method.<sup>28</sup> Briefly, HeLa cells were incubated with various concentrations of HCEE (0, 20, and 40  $\mu\text{g/mL}$ ; BD Pharmingen, Franklin Lakes, USA). Briefly, HeLa cells were trypsinized and fixed in 1% paraformaldehyde in PBS at a concentration of  $1 \times 10^6$  cells/mL. Then the cells were washed with PBS, centrifuged, resuspended in chilled ethanol overnight at  $-20^\circ\text{C}$ , washed with PBS twice, and centrifuged. Then the cells were treated with terminal deoxynucleotidyl transferase enzyme and fluorescein-conjugated deoxyuridine triphosphate, and incubated in PI/RNase staining buffer and kept under dark before analyzing by flow cytometer within 3 hours of labeling (FACSCalibur flow cytometer; BD Biosciences).

## Cell cycle analysis

Flow cytometry analysis of cell cycle was carried out to check the event of cell arrest following a previously described method.<sup>29</sup> Briefly, HeLa cells at a seeding density of  $1.5 \times 10^5$  cells/well were added into six culture plates and kept at  $37^\circ\text{C}$  for 24 hours. Then the cells were incubated with 0, 20, and 40  $\mu\text{g/mL}$  concentration of HCEE. After incubating for 24 hours, the cells were washed twice in chilled PBS, fixed with ethanol, and kept at  $-20^\circ\text{C}$ . The fixed cells were resuspended in 100  $\mu\text{g/mL}$  of RNase A and kept at  $37^\circ\text{C}$  for 30 minutes, after which the cells were stained with 50  $\mu\text{g/mL}$  of PI and kept in dark for another 30 minutes. Then the cells were subjected to analysis using a FACSCalibur flow cytometer (BD Biosciences).

## ROS assay

The production of ROS was estimated following DCFH-DA assay as previously described.<sup>30</sup> Briefly, cells at a seeding

density of  $2 \times 10^6$  cells/mL were incubated with 0, 20, and 40  $\mu\text{g/mL}$  of HCEE, followed by addition of DCFH-DA (5  $\mu\text{M}$ ) for 30 minutes at  $37^\circ\text{C}$ . Subsequently, the cells were washed with cold PBS twice and trypsinized. After that, the cell pellets were dissolved in PBS and subjected to flow cytometry detection on Becton Dickinson FACScan (Becton Dickinson Immunocytometry Systems) using Cell Quest software (BD Biosciences).

## Mitochondrial membrane potential assay

Mitochondrial membrane potential was analyzed using JC-1 dye as described previously.<sup>31</sup> HeLa cells at a concentration of  $1 \times 10^5$  cells/well were cultured overnight in six-well plates in a  $\text{CO}_2$  incubator. Cells were then incubated with 0, 20, and 40  $\mu\text{g/mL}$  of HCEE for 24 hours. Briefly, following treatment, cells were stained with 1  $\mu\text{g/mL}$  of JC-1 dye for 20 minutes at  $37^\circ\text{C}$ . Then the cells were trypsinized, washed with PBS, and observed under a fluorescence microscope (Nikon E 600; Nikon Corporation). The other aliquot of each sample was subjected to flow cytometry analysis. HeLa cells were prepared as described above. Then the cells were stained with JC-1 dye and incubated for 20 minutes at  $37^\circ\text{C}$ . Subsequently, the cells were washed twice, resuspended in 1 mL PBS, and were directly analyzed by a BD FACSCalibur using Cell Quest Pro software.

## Caspase activity assay

Caspase activity in HeLa cells exposed to HCEE was measured using specific substrates.<sup>32</sup> Briefly, HeLa cells ( $1 \times 10^6$  cells/well) were grown in six-well plates and incubated overnight in a  $\text{CO}_2$  incubator at  $37^\circ\text{C}$ . Following that, the cells were treated with different concentrations of HCEE (0, 20, and 40  $\mu\text{g/mL}$ ) and incubated for 24 hours. Subsequently, the cells were centrifuged, lysed, and incubated on ice for 1 hour. To the supernatant, specific caspase substrates (Ac-DEVD-AMC for caspase-3, Ac-IETD-AMC for caspase-8, and Ac-LEHD-AMC for caspase-9) were added. Then the cells were incubated at  $37^\circ\text{C}$  for 2 hours and the caspase activity was monitored by flow cytometer (BD Biosciences).

## Cell invasion assay

Invasion assay was performed in matrigel chambers (matrigel BD Biosciences, 6.5 mm diameter, 8  $\mu\text{m}$  pore size). Briefly, HeLa cells ( $3 \times 10^6$  cells/well) were added to 200  $\mu\text{L}$  of serum-free media and cultured for 4 hours. Briefly, HeLa cells ( $3 \times 10^6$  cells/well) were added to 200  $\mu\text{L}$  of serum-free media and cultured for 4 hours. Then the cells incubated with HCEE at various concentrations (0, 20, and 40  $\mu\text{g/mL}$ ) were

added to the upper chamber. Media supplemented with 10% FBS were kept in the lower chamber. Chambers were then assembled and incubated for 24 and 48 hours at 37°C. Fixation was carried out with 4% paraformaldehyde for 5 minutes, followed by staining with 0.5% crystal violet for 30 minutes. The noninvading cells in the upper membrane surface were scraped off using a cotton swab, and the invading cells that migrated to the lower membrane surface were randomly counted using a light microscope. Data were collected from three independent experiments.

### Cell migration assay

Wound healing assay was carried out to investigate the migration ability of HCEE on HeLa cells.<sup>33</sup> HeLa cells at a seeding density of  $5 \times 10^4$  cells/well were plated on 24-well plates and cultured until 80% confluency was reached. A linear wound was generated in the cellular monolayer using the tip of the pipette and the detached cells were removed and transferred to serum-free medium. Then the cells were incubated with control (DMSO) and various concentrations of HCEE (20 and 40  $\mu\text{g/mL}$ ). The scratch wound randomly picked from each field was photographed under a Nikon Eclipse TE2000-E microscope (Nikon Corporation) after 24 and 48 hours of incubation. The experiments were performed in triplicate. Cell migration was calculated as the migration rate (%), where

$$\text{Migration rate (\%)} = \frac{\text{Width of original wound} - \text{Width of new wound}}{\text{Width of original wound}} \times 100$$

### Gelatinase zymography

The activity of matrix metalloproteinases (MMPs) was determined using gelatin zymography.<sup>33</sup> Briefly, HeLa cells at a seeding density of  $3 \times 10^5$  cells/well were placed on six-well plates and cultured until confluency reached about 80%. Subsequently, the HeLa cells were incubated with various concentrations of HCEE for 24 hours. The supernatant was then collected and separated by SDS-PAGE under non-reducing conditions. The gel was washed with 2.5% Triton X-100 and incubated in substrate buffer (50 mM Tris-HCl, pH 7.4, and 10 mM  $\text{CaCl}_2$ ) overnight. Staining of gels was done with 0.1% Coomassie Brilliant Blue R-250 followed by destaining. Band intensity was quantified using ImageJ software.

### Western blotting

HeLa cells ( $3 \times 10^5$  cells/well) were seeded in six-well culture plates and incubated with various concentrations of HCEE

(0–40  $\mu\text{g/mL}$ ) for 24 hours. After 24 hours, cells were lysed with buffer containing 50 mM Tris-HCl, 150 mM NaCl, 1% Triton X-100, 1% NP-40, 10  $\mu\text{L/mL}$  phosphatase inhibitor cocktail and protease inhibitor cocktail. Lysed cells were collected and centrifuged for 10 minutes at 4°C. The protein content was estimated by bicinchoninic acid assay; 40  $\mu\text{g}$  of the extracted protein was separated on 10% SDS-PAGE gels (w/v) and then transferred onto 0.45  $\mu\text{m}$  polyvinylidene difluoride membrane. Membranes were then blocked in 4% BSA in Tris buffer saline containing 0.1% of Tween-20. After blocking at 37°C for 1 hour, the membrane was probed with primary antibodies overnight at 4°C. The following primary antibodies were used: those involved with cell cycle, such as anti-p53, anti-p21, anti-CDK4, anti-CDK6, and anti-cyclin D1; those associated with apoptosis, such as anti-apoptosis protease-activating factor 1 (anti-Apaf-1), anti-bax, anti-cytochrome *c*, anti-bcl-2, anti-Fas, and anti-FasL; and those associated with cell migration and invasion, such as anti-MMP2, anti-MMP9, and anti- $\beta$  actin antibody.  $\beta$ -actin was used as a reference gene. After washing the membrane with Tween buffer, it was incubated at 37°C for 2 hours with appropriate anti-mouse secondary antibody conjugated to HRP (1:10,000). Immunoreactive bands were detected using enhanced chemiluminescence reagent (EMD Millipore, Billerica, MA, USA).

### Statistical analysis

All the results are represented as mean  $\pm$  SD (n=3). Statistical analysis was done using GraphPad Prism software 7. Difference between groups was tested by one-way ANOVA followed by Tukey's multiple comparison test at  $*P < 0.05$ ,  $**P < 0.01$ , and  $***P < 0.001$ .

## Results

### Analysis of constituents by HPLC

*H. coronarium* with its several labdane diterpenes is known for their cytotoxic and anti-inflammatory activity, and hence, we tried to characterize the constituents present in HCEE by HPLC. The major constituents in HCEE were found to be coronarin-D methyl ether (Rt=4.12 minutes) and coronarin-D (Rt=5.42 minutes), as shown in Figure 1A. The confirmation was done by comparing their retention time with their respective standards (Figure 1B). Linear regression equation was obtained by plotting the area units in Y-axis against the concentration in X-axis. Based on the linear regression, the amounts of coronarin-D and coronarin-D methyl ether in HCEE were estimated to be 46.8 and 6.21 mg/100 g, respectively.

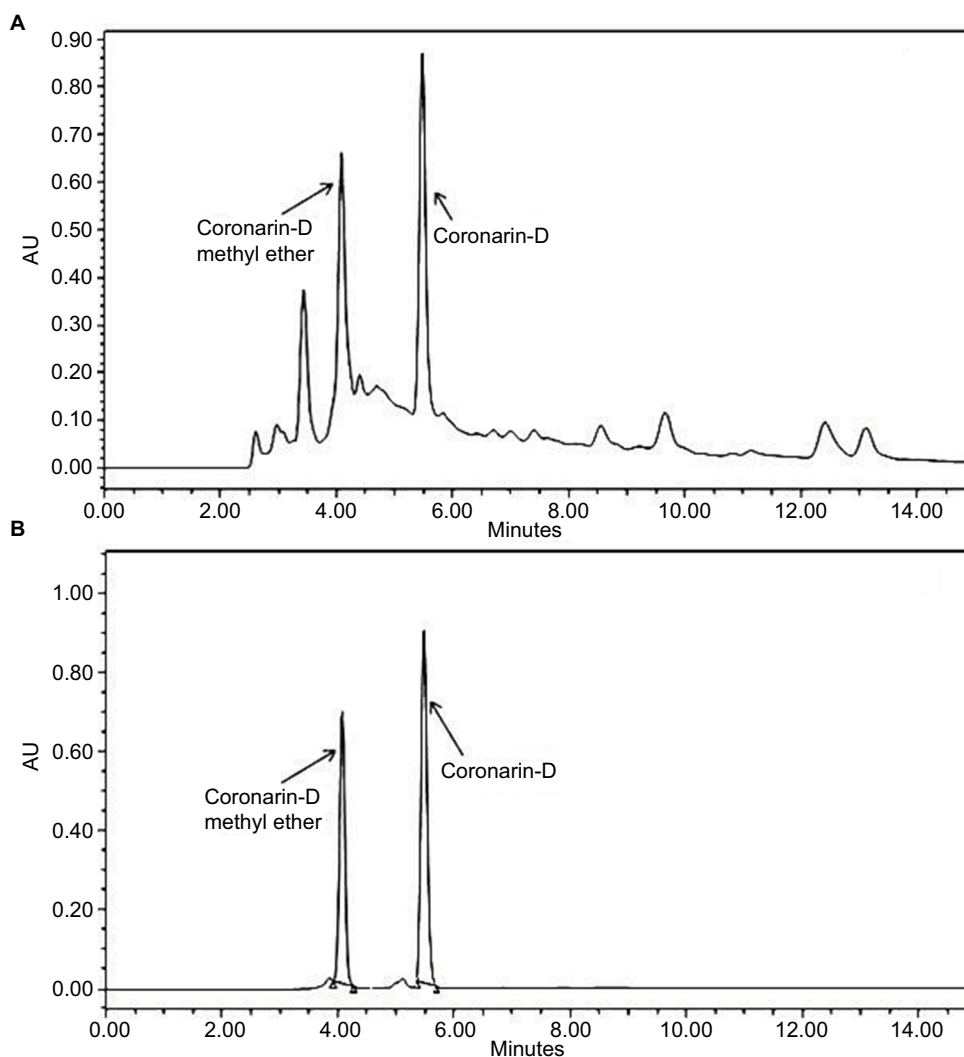


**Figure 1** HPLC chromatograms of (A) HCEE and (B) coronarin-D methyl ether standard ( $R_t=4.12$  minutes) and coronarin-D ( $R_t=5.42$  minutes).  
**Abbreviations:** AU, area units; HCEE, *Hedychium coronarium* ethanol extract.

## Cytotoxic effects of HCEE on HeLa cells

The cytotoxic effect of HCEE was evaluated on A549, HeLa, PANC-1, LnCaP, Jurkat, and HUVEC cells by MTT assay. Briefly, cells were incubated with various concentrations of HCEE (1, 10, 20, 40, 80, 160, and 320  $\mu\text{g}/\text{mL}$ ) for 24, 48, and 72 hours. Table 1 depicts the  $IC_{50}$  value of all the cell lines for 24, 48, and 72 hours. Among the selected cell lines, HeLa cells were the most sensitive to HCEE with  $IC_{50}$  values of  $17.18 \pm 0.46$ ,  $15.32 \pm 0.68$ , and  $12.57 \pm 0.32$   $\mu\text{g}/\text{mL}$  after 24, 48, and 72 hours of incubation, respectively. Unexpectedly, HCEE had lesser cytotoxic activity against A549, PANC-1, LnCaP, and Jurkat cells with  $IC_{50}$  values greater than 100  $\mu\text{g}/\text{mL}$ . The observed decrease in the  $IC_{50}$  values with corresponding increase in incubation time suggests a time-dependent inhibitory effect of the drug (HCEE) on all cells. Camphothecin, a standard anticancer drug, was used

as a positive control. From Table 1, it can be observed that camphothecin was toxic not only against cancerous cells but also toward normal HUVEC cells. In contrast, selective cytotoxicity ( $IC_{50}$  values  $>320$   $\mu\text{g}/\text{mL}$ ) was observed in normal HUVEC cells, which confirmed that HCEE is nontoxic toward normal cells.

The ability of HeLa cells to survive after treatment with HCEE was further determined using clonogenic survival assay. As shown in Figure 2A, the survival fraction of HeLa cells was significantly reduced to 37.9% and 12.6% at 20 and 40  $\mu\text{g}/\text{mL}$  of HCEE, respectively. With increasing concentration of the HCEE (20 and 40  $\mu\text{g}/\text{mL}$ ), there was a significant reduction of colonies as compared to untreated cells (control), as shown in Figure 2B. These results demonstrated that HCEE reduces the survival of HeLa cancer cell lines.

**Table 1** IC<sub>50</sub> values (expressed as µg/mL) in tested cancer (A549, HeLa, PANC-1, LnCaP, Jurkat) and normal (HUVEC) cell lines treated with the investigated samples: HCEE and positive control camphothecin

Cell name	Incubation (hours)	IC <sub>50</sub> value (µg/mL)	
		HCEE	Camphothecin
A549	24	148.34±2.11	3.74±0.18
	48	119.41±1.37	3.19±0.21
	72	103.67±2.24	2.83±0.29
HeLa	24	17.18±0.46	0.98±0.11
	48	15.32±0.68	0.87±0.21
	72	12.57±0.32	0.82±0.15
PANC-1	24	166.32±3.64	0.69±0.08
	48	141.51±2.87	0.57±0.03
	72	129.76±2.13	0.51±0.06
LnCaP	24	197.28±5.08	6.12±0.34
	48	184.43±4.19	4.83±0.37
	72	171.55±4.52	4.19±0.43
Jurkat	24	156.28±4.78	2.32±0.21
	48	132.19±3.61	1.96±0.26
	72	119.13±2.87	1.64±0.09
HUVEC	24	>320	10.13±0.62
	48	247.64±4.61	9.83±0.51
	72	211.39±5.03	9.19±0.35

**Note:** Values are mean ± SD of three determinations.

**Abbreviations:** HCEE, *Hedychium coronarium* ethanol extract; HUVEC, human umbilical vein endothelial cell.

## HCEE induced apoptosis in HeLa cells

The HeLa cells stained with DNA-specific dye, Hoechst 33342, were examined for morphologic changes (Figure 3A). The cell samples of HCEE-treated cells (20 and 40 µg/mL) and the control (0.1% DMSO)-treated HeLa cells were compared. Control cells exhibited less bright blue fluorescence with intact round nuclei, whereas extract-treated cells stained with Hoechst 33342 showed bright fluorescence and exhibited characteristic feature of apoptosis, such as cell shrinkage, chromatin condensation, and nuclear fragmentation. The frequency of apoptosis increased with a corresponding dose-dependent increase in HCEE.

In order to confirm whether cells undergo apoptosis, we measured the apoptotic cells percentage by Annexin V-FITC/PI dual-labeling assay. Flow cytometry analysis of stained cells could distinguish the cells into four groups, namely, viable (Annexin V-PI-), early apoptosis (Annexin V+PI-), late apoptosis (Annexin V+PI+), and necrotic (Annexin V-PI+) cells. As presented in Figure 3B, there was a significant increase in percentage of late apoptosis and early apoptosis cells after incubation with different concentrations of the HCEE extract for 24 hours. The percentage of late apoptotic cells increased significantly with increasing doses of HCEE:

48.30% (20 µg/mL) and 59.35% (40 µg/mL), compared to the control group (8.20%). Similarly, the percentage of early apoptotic cells also increased to 6.35% (20 µg/mL) and 8.40% (40 µg/mL), respectively, as compared to the control group (0.65%), as shown in Figure 3C. Less than 8% of the population showed necrotic signs when treated with 20 and 40 µg/mL of HCEE.

## HCEE increased TUNEL-positive cells

The extent of apoptotic DNA degradation was analyzed by TUNEL assay. There was an increase in fluorescence shift toward the left in HeLa cells incubated with HCEE, thus showing an increase in percentage of TUNEL-positive cells (Figure 4). The TUNEL-positive cells increased from 1.07% in the control to 22.67% and 62.59% for 20 and 40 µg/mL of HCEE, respectively.

## HCEE induced G1 phase cell cycle arrest in HeLa cells

Flow cytometry was used to investigate the effect of HCEE on HeLa cell cycle distribution in different phases after incubation for 24 hours (Figure 5A). As represented in Figure 5B, the proportion of HeLa cells in G1 phase increased from 45.61%±1.10% in the control to 57.92%±1.30% and 64.66%±1.60% in 20 and 40 µg/mL of HCEE, respectively. In addition, HCEE caused a reduction in percentage of cells in G2/M phase from 45.20%±1.30% in the control to 29.25%±1.10% and 22.56%±0.80% in 20 and 40 µg/mL of HCEE-treated cells, respectively (Figure 5B). A marked increase in the G1 phase cells was accompanied by a decrease in the G2/M phase cells. This finding makes us assume that HCEE-induced apoptosis may be associated with cell cycle arrest at the G1 phase.

## HCEE leads to ROS generation in HeLa cells

DCFH-DA assay was carried out to monitor the changes in levels of ROS on exposure of HeLa cells to various concentrations of HCEE for 24 hours (Figure 6A). As shown in Figure 6B, treatment of HeLa cells with HCEE at concentrations of 20 and 40 µg/mL significantly increased the ROS levels to 48% and 60%, respectively, compared to control. To understand the role of ROS in HCEE-induced cytotoxicity, we checked whether an antioxidant, NAC, could protect HeLa cells against HCEE-induced cytotoxicity. Treatment with NAC inhibited the production of ROS and significantly reduced the death of HeLa cells induced by HCEE. The cell viability was assessed by MTT assay (Figure 6C). The

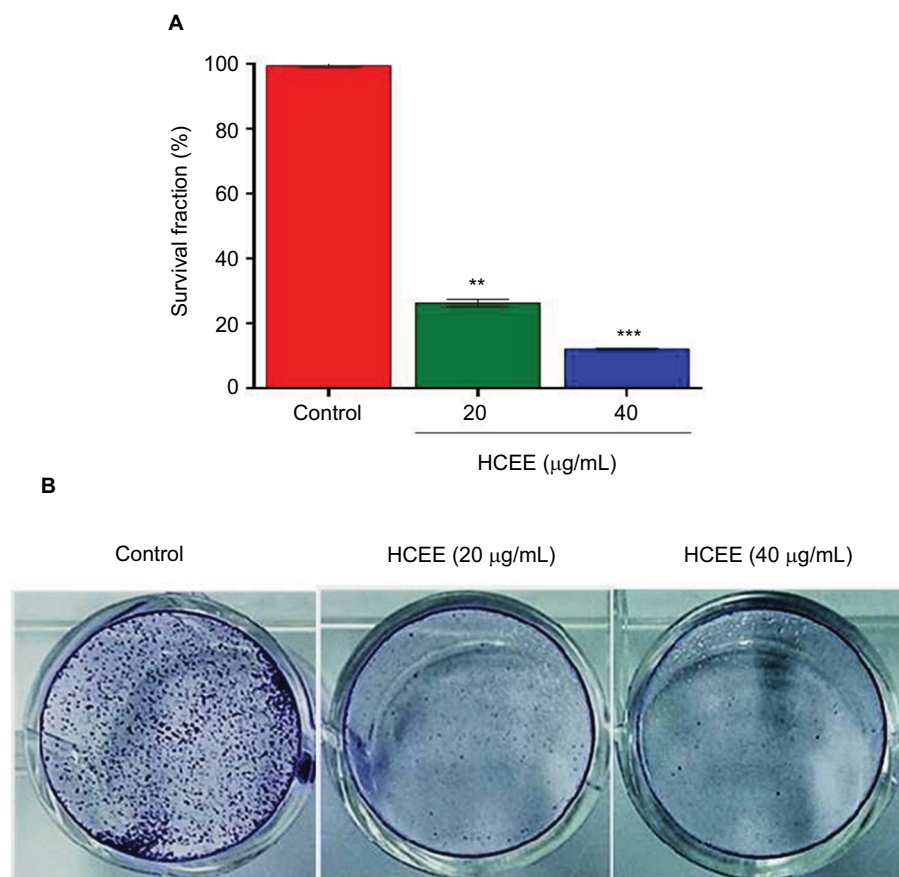


**Figure 2** Effect of HCEE on the clonogenic survival of cervical cancer HeLa cells.

**Notes:** (A) HeLa cells were seeded on six-well plates and incubated overnight. Then the cells were treated with 0, 20, and 40 µg/mL of HCEE for 48 hours. After incubation for 7 days, the colonies were stained with methylene blue after which they were fixed with methanol and imaged under a microscope. (B) Representative histograms are expressed as survival fraction and represent the mean  $\pm$  SD of three different experiments ( $n=3$ ). \*\* $P<0.01$  and \*\*\* $P<0.001$  denotes statistically significant difference between the control and treated groups.

**Abbreviation:** HCEE, *Hedychium coronarium* ethanol extract.

findings indicate ROS generation to be a possible cause of HCEE-induced cell death.

### HCEE induced depolarization of mitochondrial membrane potential

In order to assess the mitochondrial damage due to cell death, changes in mitochondrial membrane potential were monitored following staining with mitochondrial-specific JC-1 dye. In undamaged mitochondria with high membrane potential, JC-1 forms aggregates (red fluorescence) in live cells, whereas in apoptotic cells (green fluorescence), it forms monomer with low mitochondrial membrane potential (Figure 7A). Treatment of HeLa cells with increasing concentration of HCEE (20 and 40 µg/mL) showed a decrease in red to green fluorescence as compared to control, thus suggesting a loss of membrane potential. To investigate the quantitative analysis of mitochondrial membrane potential,

flow cytometry analysis was carried out (Figure 7B). Treatment with increasing concentrations of HCEE decreased the ratio of aggregate/monomer from 11.93 (control) to 0.84 (20 µg/mL) and 0.13 (40 µg/mL), respectively (Figure 7C). The results suggest that HCEE induced a loss of mitochondrial membrane potential in HeLa cells.

### HCEE promoted extrinsic and intrinsic pathways through activation of caspases in HeLa cell lines

In order to study the role of caspases in HCEE-induced apoptosis, the levels of active caspase-3, caspase-8, and caspase-9 in HeLa cells treated with different concentrations of HCEE for 24 hours were measured by flow cytometry (Figure 8A). As shown in Figure 8B, the fluorescence intensity of active caspase-3, caspase-9, and caspase-8 increased following treatment with HCEE (20 and 40 µg/mL). The results suggest

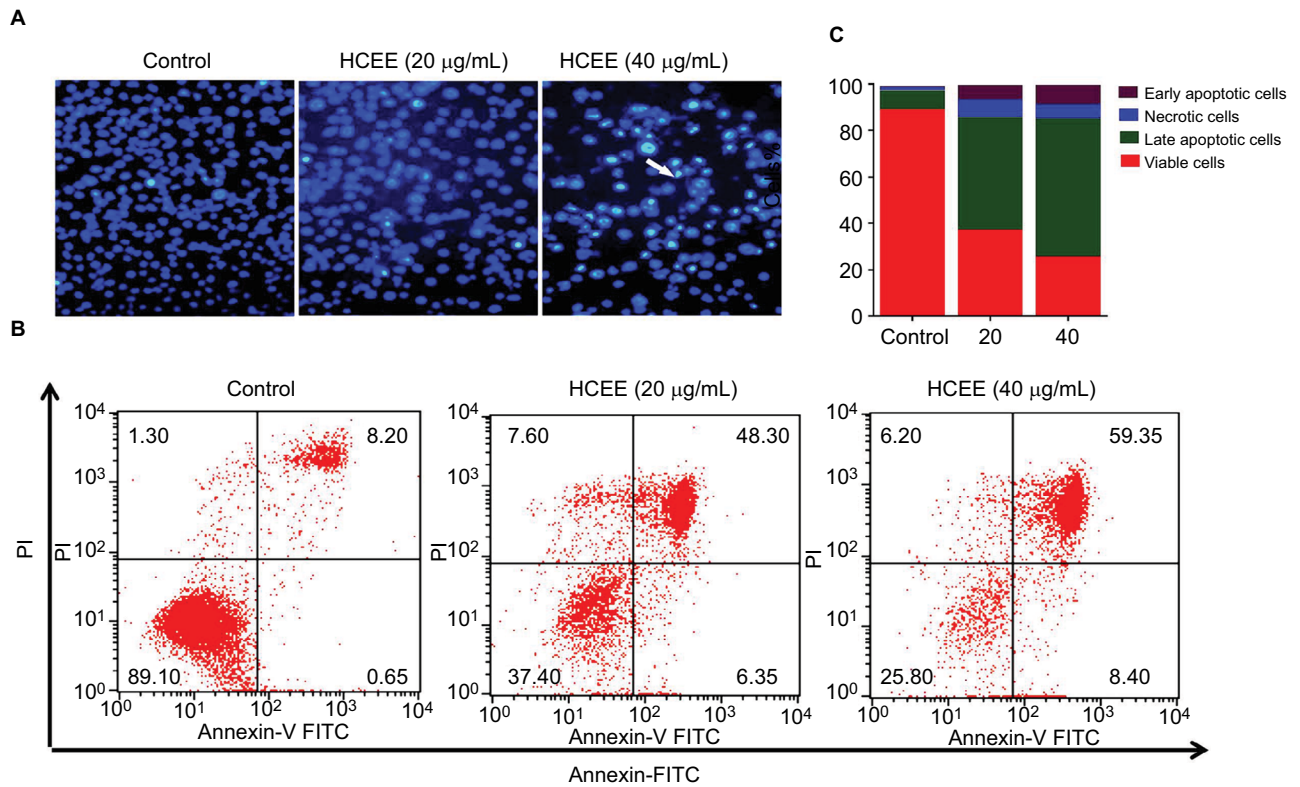


**Figure 3** Effect of HCEE-induced cell apoptosis in HeLa cells.

**Notes:** (A) Fluorescent assay of Hoechst 33342 staining. HeLa cells were treated with different concentrations (0, 20, and 40 µg/mL) of HCEE, followed by staining with Hoechst 33342 staining solution and visualization under a fluorescent microscope. (B) Flow cytometry analysis of cell apoptotic rates using Annexin V-FITC/PI double labeling. (C) The percentage of live, early apoptotic, late apoptotic, and necrotic cells at different concentrations (0–40 µg/mL) of HCEE. Data are mean ± SD from three individual experiments.

**Abbreviations:** FITC, fluorescein isothiocyanate; HCEE, *Hedychium coronarium* ethanol extract; PI, propidium iodide.

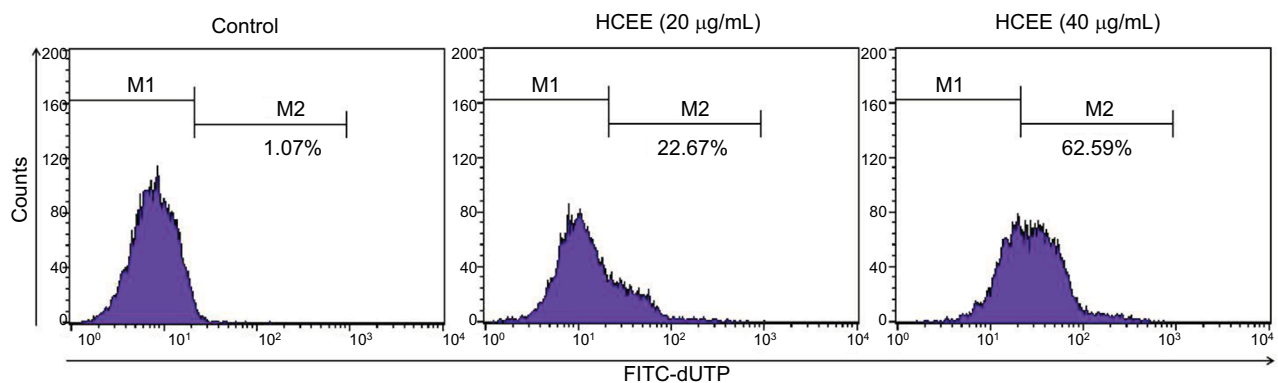


**Figure 4** Effect of HCEE on DNA fragmentation in HeLa cells as measured by TUNEL assay.

**Notes:** HeLa cells were incubated for 24 hours with various concentration of HCEE (0–40 µg/mL). They were then treated with DNA labeling solution containing terminal deoxynucleotidyl transferase enzyme and fluorescein-conjugated dUTP and further incubated in PI/RNase staining buffer and kept under dark before analyzing by flow cytometry. Representative dot plot image shows the fluorescence shift toward the left, thereby indicating the increase in TUNEL-positive cells.

**Abbreviations:** dUTP, deoxyuridine triphosphate; FITC, fluorescein isothiocyanate; HCEE, *Hedychium coronarium* ethanol extract; PI, propidium iodide.

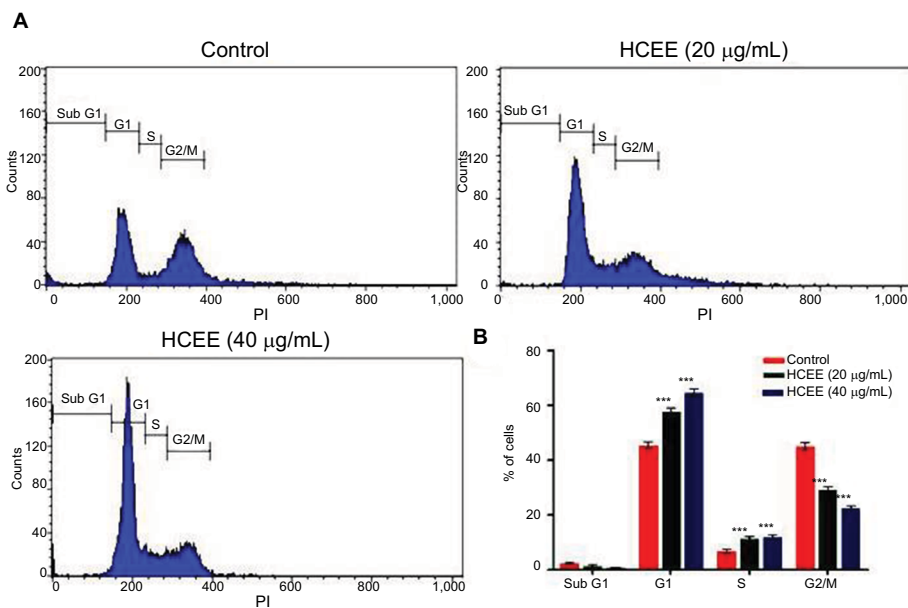


**Figure 5** Effect of cell cycle distribution of HeLa cells exposed to different concentrations of HCEE (0–40 µg/mL) for 24 hours. **Notes:** (A) Flow cytometric analysis of cell cycle with PI DNA staining. (B) The percentage of cell cycle distribution in different phases of cell cycle. Data are represented as mean ± SD of three independent experiments. The significant differences in treated cells and the control group are shown by \*\*\* $P < 0.001$ . **Abbreviations:** HCEE, *Hedychium coronarium* ethanol extract; PI, propidium iodide.

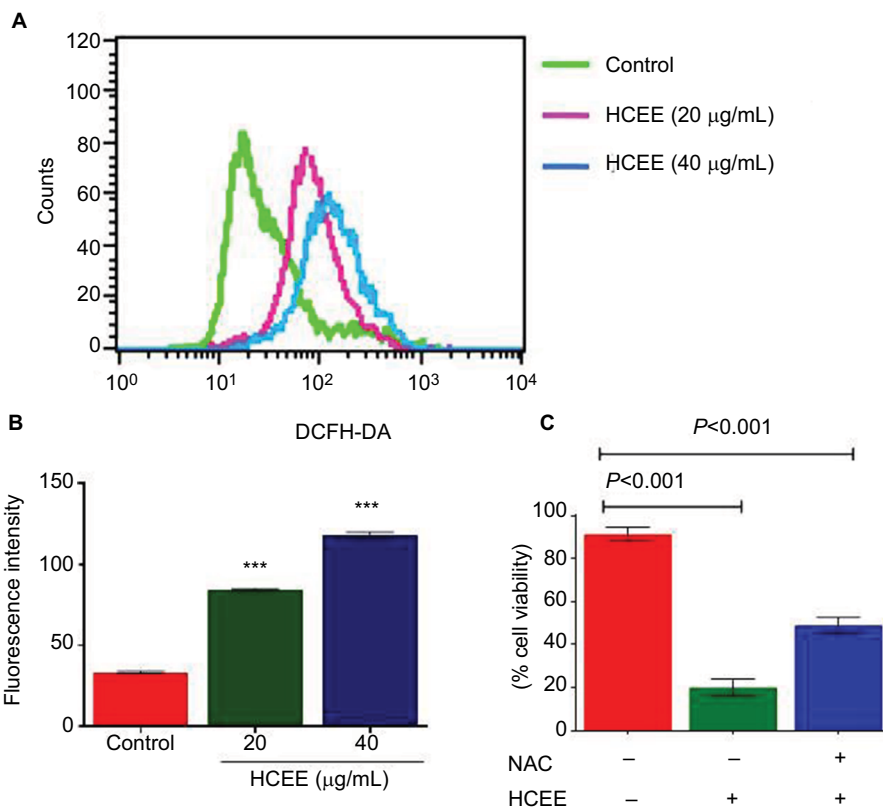


**Figure 6** Effect of HCEE on ROS generation in HeLa cells. **Notes:** (A) HeLa cells were treated with control, 20 and 40 µg/mL of HCEE and stained with DCFH-DA. Then they were subjected to flow cytometry. (B) Histogram of mean fluorescence intensity of DCFH-DA-stained HeLa cells exposed to control and various concentrations of HCEE (20 and 40 µg/mL). Each value represents mean ± SD (n=3). \*\*\* $P < 0.001$  compared with control. (C) HeLa cells were treated with 20 µg/mL of HCEE in the presence or absence of 10 mM NAC for 24 hours. Cell viability was measured using MTT assay and the results are represented as mean ± SD (n=3). \*\*\* $P < 0.001$  vs control group. **Abbreviations:** DCFH-DA, 2',7'-dichlorodihydrofluorescein diacetate; HCEE, *Hedychium coronarium* ethanol extract; NAC, N-acetyl-L-cysteine.

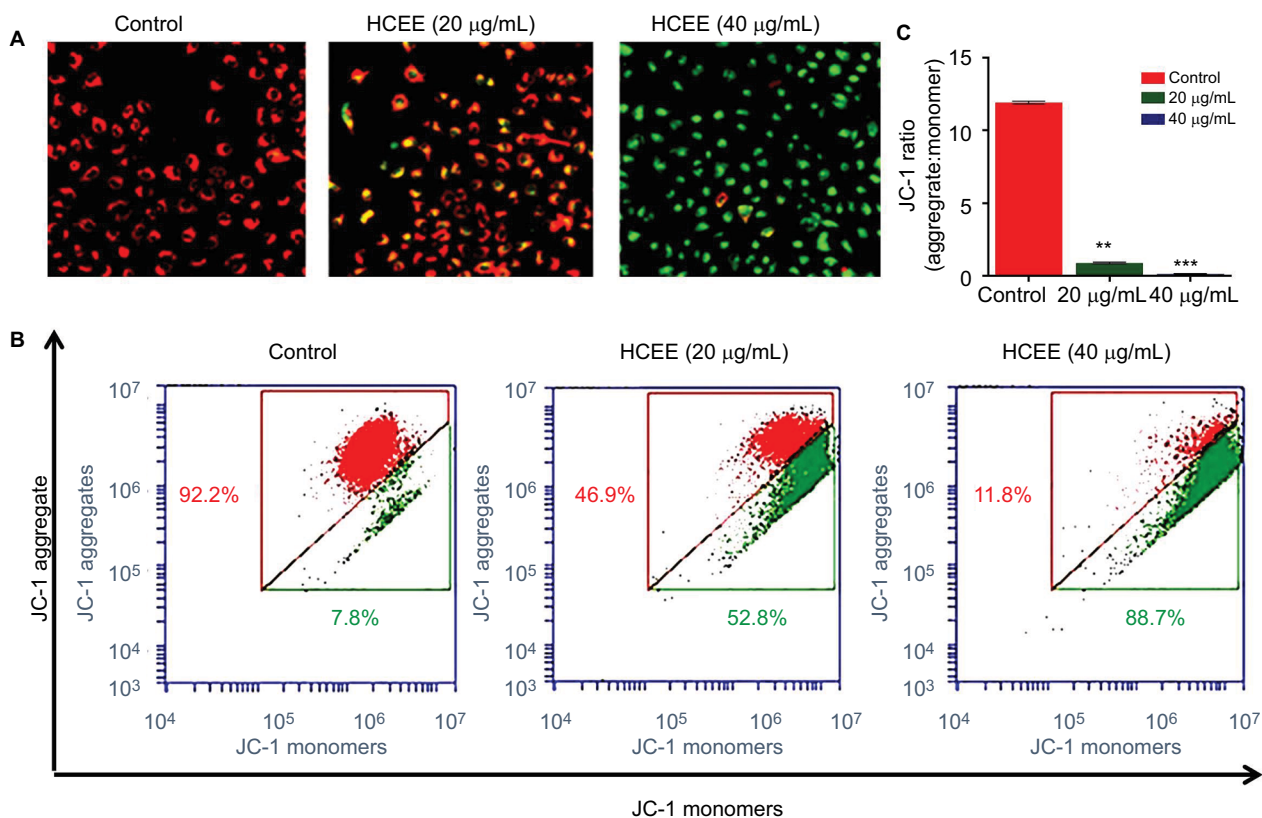


**Figure 7** Mitochondrial membrane potential of HeLa cells treated with HCEE as determined by JC-1 fluorescent dye.

**Notes:** (A) Representative images of JC-1 staining in HeLa cells treated with different concentrations of HCEE (0–40 µg/mL). After 24 hours, the cells were stained with JC-1 probe and imaged under fluorescence microscope, which showed loss of red fluorescence (aggregate) and abundance of green fluorescence (monomers), thereby indicating depolarization of mitochondrial membrane potential. (B) Evaluation of mitochondrial membrane potential in HeLa cells by flow cytometry. (C) Quantification of mitochondrial membrane potential (% of control) was expressed as JC-1 ratio (aggregate:monomer). Data represent mean  $\pm$  SD of three replicates. \*\* $P < 0.01$ , \*\*\* $P < 0.001$  vs control group.

**Abbreviation:** HCEE, *Hedychium coronarium* ethanol extract.

that HCEE initiates apoptosis by activation of caspases involved in both cell extrinsic and intrinsic pathways.

### HCEE inhibited migration and invasion of HeLa cells through downregulation of MMP-2 and MMP-9 expression

To examine the antimetastatic activity of HCEE on invasion of HeLa cells, Transwell invasion assay was performed (Figure 9A). HCEE restricted the invasion of HeLa cells through the Matrigel basement membrane in a concentration-dependent manner. HeLa cells incubated in 20 and 40 µg/mL of HCEE extract for 24 hours showed decrease in invasion to 81% $\pm$ 1% and 63% $\pm$ 0.8%, respectively, compared to control (Figure 9B). The cell invasion in HeLa cells treated with 20 and 40 µg/mL of HCEE after 48 hours was reduced to 80% $\pm$ 1.1% and 52% $\pm$ 0.9%, respectively, compared to control.

Further, to evaluate the effect of HCEE on HeLa cells' migration, wound healing assay was performed (Figure 9C). It was found that treatment with HCEE significantly

decreased the migration rate of HeLa cells after 24 and 48 hours in a concentration-dependent manner (Figure 9D). Treatment with HCEE at a concentration of 20 and 40 µg/mL showed decrease in migration rate to 79% $\pm$ 0.8% and 62% $\pm$ 0.5%, respectively, compared to that of control (DMSO treated) after 24 hours. Similarly, cells treated with 20 and 40 µg/mL of HCEE after 48 hours of incubation showed decrease in cell migration to 74% $\pm$ 0.6% and 48% $\pm$ 0.9%, respectively, compared to that of control. Further, the inhibitory effect of HCEE extract on MMP production was assessed by gelatin zymography (Figure 9E). As shown in Figure 9F, there was a reduction in activity of MMP-2 and MMP-9 with increasing concentration of HCEE after 24 hours. The result suggests that HCEE might suppress the invasion and metastasis of HeLa cervical cancer cells by reducing the activities of MMP-2 and MMP-9, respectively. These results discussed here could indicate that HCEE attenuates the migration and invasion of HeLa cervical cancer cells in vitro.

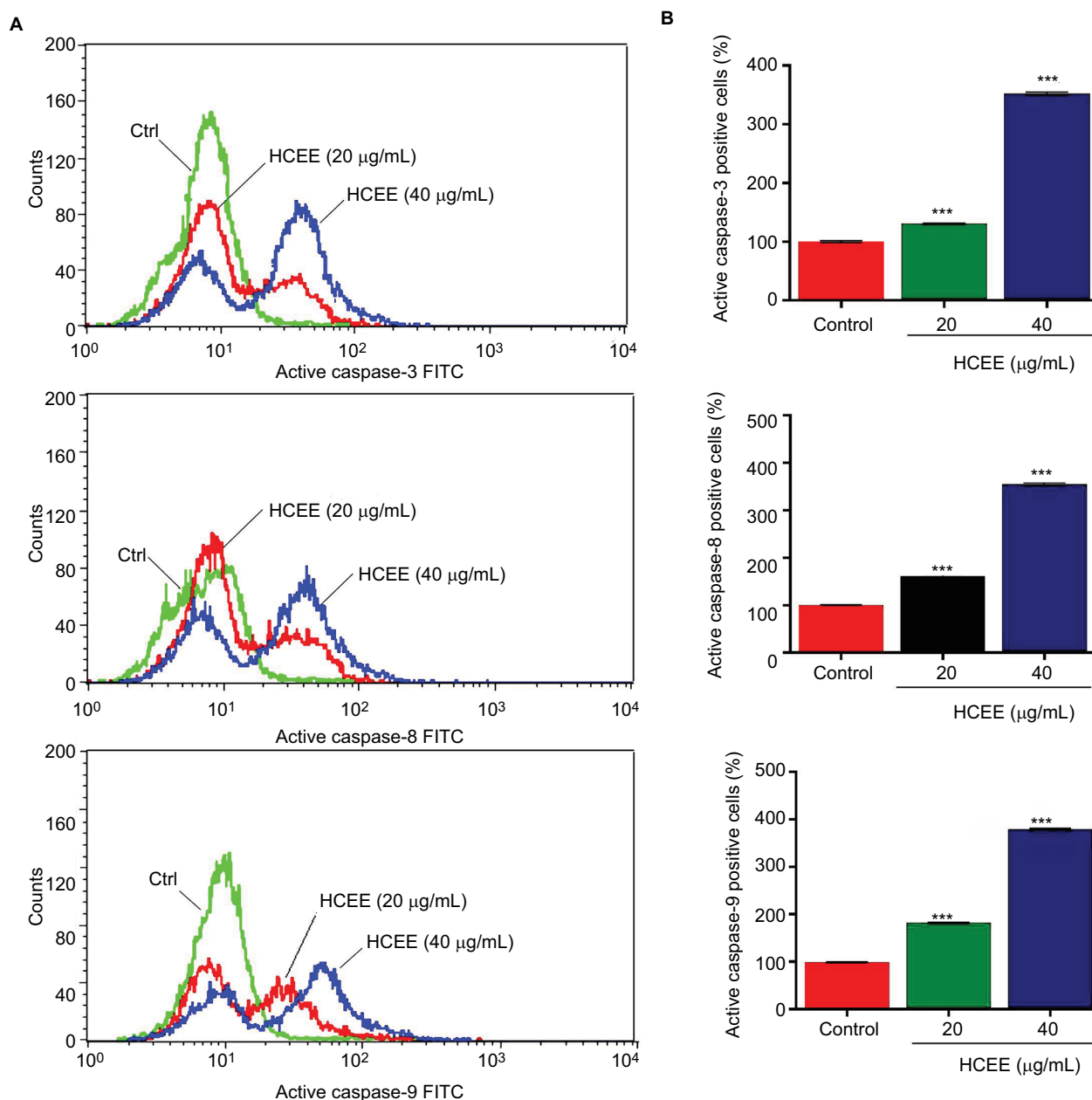


**Figure 8** Effect of HCEE on activation of caspases.

**Notes:** (A) Flow cytometry analysis of active caspase-3, caspase-8, and caspase-9 in HeLa cells. (B) Quantitative analysis of apoptotic cell population for active caspase-3, caspase-8, and caspase-9. Data are represented as mean  $\pm$  SD values of three experiments. \*\*\* $P < 0.001$  compared with untreated control group.

**Abbreviations:** FITC, fluorescein isothiocyanate; HCEE, *Hedychium coronarium* ethanol extract.

## HCEE alters the expression levels of proteins associated with cell cycle, apoptosis, migration, and invasion in HeLa cells

In order to understand the mode of HCEE-induced apoptotic cell death in HeLa cells, the expression level of proteins involved in mitochondrial-associated and death receptor

pathway was checked. The results of Western blotting analysis showed increased expression of Fas ligand (FasL) and Fas receptor (Fas). Similarly, the results of Western blotting demonstrated that increasing concentration of HCEE decreased the expression levels of antiapoptotic protein Bcl-2 and elevated the levels of proapoptotic protein Bax in HeLa cells (Figure 10A and 10E). The results confirmed that HCEE promoted extrinsic and mitochondrial apoptotic signaling

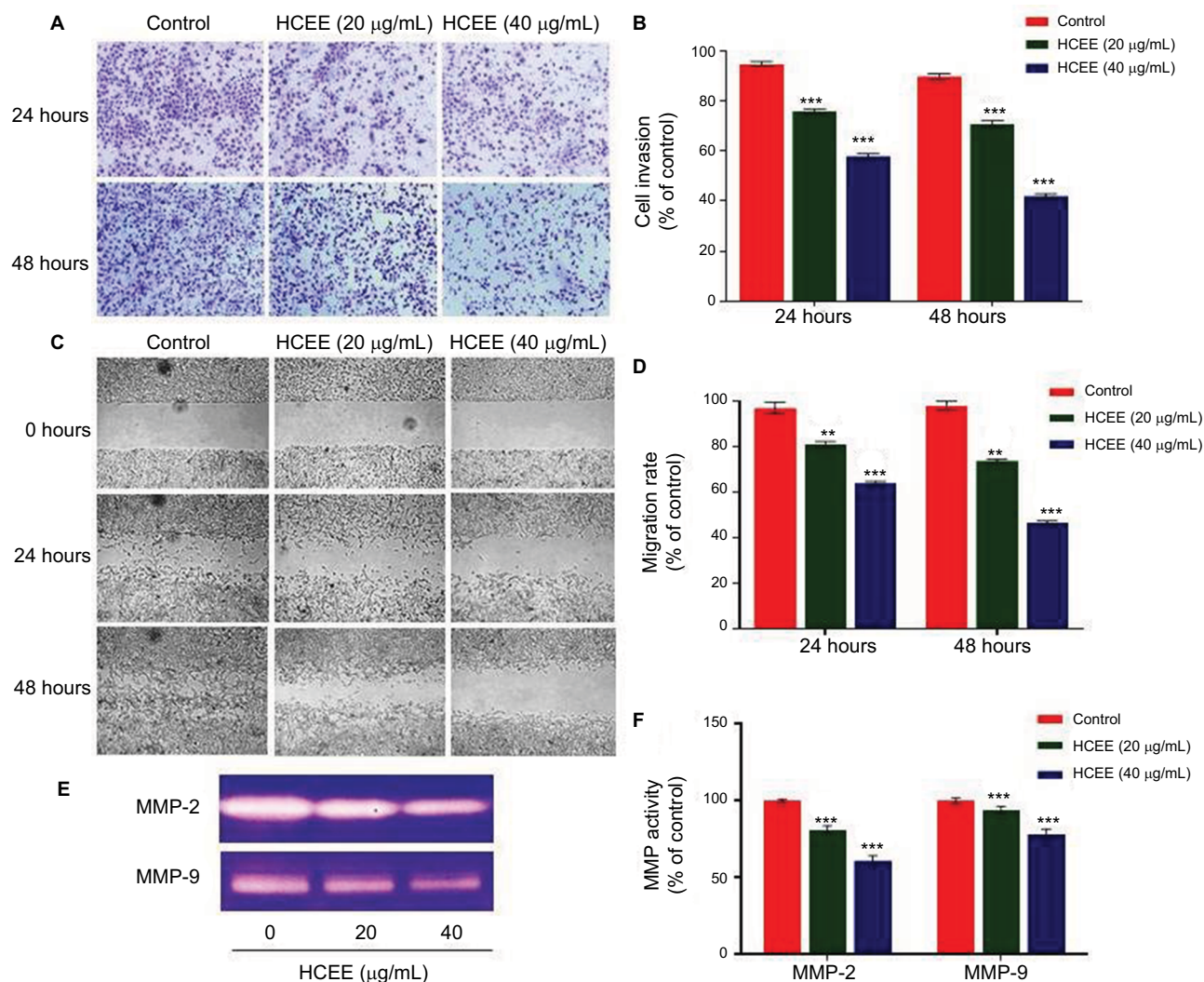


**Figure 9** Effect of HCEE on HeLa cells' migration and invasion in vitro.

**Notes:** (A) Representative images of HeLa cell invasion treated with HCEE and examined by the Transwell invasion assay. Magnification 10 $\times$ . (B) Quantitative analysis of percent of cell invasion in HCEE-treated cells compared to the control. Data are representative of three replicates and are expressed as mean  $\pm$  SD. \*\*\* $P$ <0.001 compared with control group. (C) Wound closure ability of treated HeLa cells after creation of scratch wound in control and treated wells. The images of wounded extract-treated HeLa cell monolayers captured using a phase-contrast microscope at different time intervals (0, 24, and 48 hours) after the scratch are shown. Magnification 10 $\times$ . (D) Migration rates were quantitatively analyzed by calculating the difference between wound widths of HCEE-treated and control cells at 0, 24, and 48 hours. Results are expressed as percentage of cell migration. (E) MMP activity by gelatin zymography assay. (F) Quantification of gelatin zymography data for MMP-2 and MMP-9. Data were presented as mean  $\pm$  SD for three independent experiments. \*\* $P$ <0.01, \*\*\* $P$ <0.001 compared with control group. \*\* $P$ <0.01, \*\*\* $P$ <0.001 compared with control group.

**Abbreviation:** HCEE, *Hedychium coronarium* ethanol extract.

pathways. In addition, Western blot analysis also showed that treatment with HCEE led to an increase in the cytosolic levels of cytochrome *c* and Apaf-1. Further, investigation of cell cycle-associated proteins by Western blotting was done in order to evaluate the underlying mechanism of G1 phase cell arrest. As shown in Figure 10B and 10D, HCEE at both concentrations (20 and 40  $\mu$ g/mL) promoted upregulation of p53 and its effector protein p21 and decreased the expression of checkpoint protein, Cyclin D1, and its associated cyclin-dependent kinases Cdk4 and Cdk6. Further, in order to check

the migratory potential, the expression levels of MMPs were assessed. It was observed that the expression of MMP-2 and MMP-9 was significantly reduced in HeLa cells incubated with HCEE compared to the control, thus suggesting a major role of HCEE in reducing the metastasis of HeLa cervical cancer cells (Figure 10C and 10F).

## Discussion

*Hedychium* is known to be rich in several phytochemicals such as diterpenes, sesquiterpenes, diarylheptanoids,

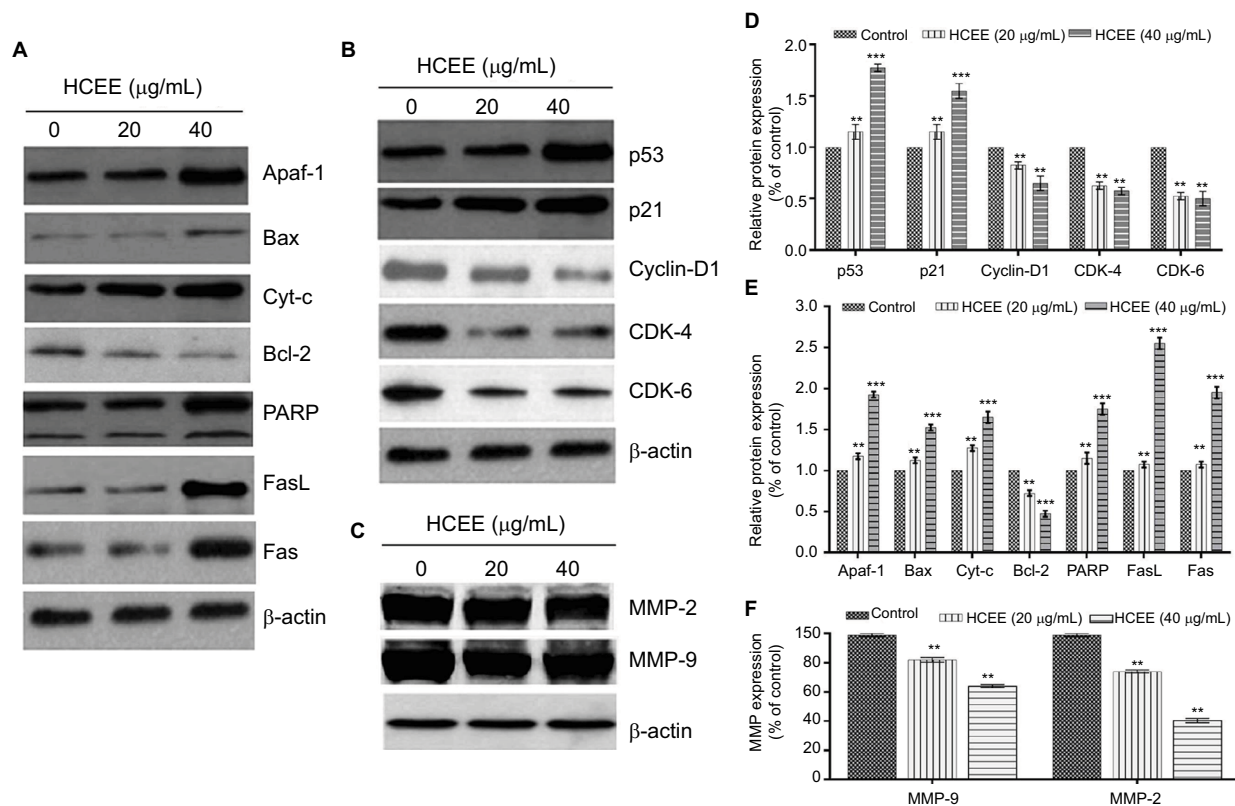


**Figure 10** Western blot analysis. Cells treated with HCEE were lysed for Western blot analysis with antibodies against (A) apoptosis, (B) cell cycle and (C) cell migration and invasion proteins. (D–F) Densitometry analysis of proteins performed using ImageJ software.

**Notes:**  $\beta$ -actin was used as a reference gene. The blots represent one typical result from three independent experiments. \*\* $P < 0.01$  and \*\*\* $P < 0.001$  were considered statistically significant differences between the control and treated groups.

**Abbreviation:** HCEE, *Hedychium coronarium* ethanol extract.

phenolic, fatty acids, and steroids.<sup>34</sup> Numerous research reports have shown labdane diterpenes to possess significant cytotoxic activity against different cancer cell lines.<sup>22,35,36</sup> HPLC analysis done in the present study showed the presence of labdane diterpenes coronarin-D and coronarin-D methyl ether in *H. coronarium* extract. Coronarin-D inhibits the NF- $\kappa$ B activation pathway which leads to inhibition of invasion and inflammation.<sup>37</sup> Another study has shown coronarin-D methyl ether to display strong cytotoxic activity against human neuroblastoma SK-N-SH cell line.<sup>23</sup> Coronarin-D also displayed pronounced cytotoxicity against HuCCA-1, MOLT-3, HeLa, and P388 cell lines.<sup>38</sup> HCEE was tested for its cytotoxicity effect on different cancer cell lines. The  $IC_{50}$  values obtained for different cell lines showed that HeLa cells were more sensitive to HCEE. Interestingly, HCEE exhibited selective cytotoxicity on normal human HUVEC cell line. The ability of antineoplastic activity of the extract to discriminate between normal and malignant cells is a crucial paradigm in the discovery of effective chemotherapeutic

agents because the currently available drugs reportedly target normal as well as cancerous cells.

These data are additionally supported by clonogenic survival assay which showed a significant decrease in the number of colonies compared to that of untreated cells (control), thus confirming the antineoplastic activity of HCEE against HeLa cells. Induction of apoptosis by HCEE was validated by several changes in cellular morphology as observed by the Hoechst 33342 staining assay. HeLa cells showed bright fluorescence and exhibited distinct apoptotic features such as cell shrinkage, condensation of chromatin, and nuclear membrane blebbing following treatment with HCEE. Several reports have revealed that phosphatidylserine, which is localized in the inner plasma membrane lipid, flips out to the outer membrane leaflet and provides stimulus for production of anti-inflammatory mediators during the early apoptotic stages.<sup>39,40</sup> In addition to Hoechst 33342 staining assay, Annexin V assay also suggested that the primary cause of cell death following HCEE treatment was apoptosis and

the effect was dose dependent. TUNEL assay also showed fluorescence shift toward the left, thereby showing an increase in TUNEL-positive cells following treatment with HCEE.

Numerous reports have shown that cell cycle arrest and apoptosis are interconnected.<sup>41,42</sup> Deregulation of cell signaling pathways leads to cancer initiation, and hence, targeting cell cycle proteins has emerged as a potential tool for cancer therapeutics.<sup>43</sup> It is also widely recognized that DNA damage could cause an increase in level of tumor suppressor protein p53 to induce cell cycle arrest at G1, G2, or S phase and enable DNA repair to take place.<sup>44,45</sup> p21, a cyclin-dependent kinase inhibitor, is upregulated by p53 upon cellular stress or DNA damage. Overexpression of p21 can cause cell cycle arrest via interaction with a wide range of cyclin/CDK complexes.<sup>46</sup> Therefore, activation of p21 mediated by p53 is an important key in altering cancer cell growth. The kinase activity of CDKs is regulated by interaction with their catalytic subunit cyclin, binding to negative inhibitors, and also through regulatory phosphorylation and dephosphorylation.<sup>47</sup> Therefore, in the present research, we performed DNA damage and measured the expression levels of p53 and p21. As expected, after the HeLa cells were treated with HCEE for 24 hours, the cell cycle was arrested at G1 phase via activation of p53 and p21. Therefore, we suggest that the growth inhibition of HCEE was associated with G1 phase arrest, which was related to p53-dependent regulation in HeLa cells.

Multiple lines of evidence suggest that mitochondrial-derived ROS are the early inducers of autophagy upon nutrient starvation.<sup>48–50</sup> Accumulation of ROS induces mitochondrial destabilization, thereby promoting apoptosis. As evident from the DCFH-DA assay, there was an increase in the formation of intracellular ROS on incubation of HeLa cells with HCEE. DCFH-DA is a free radical indicator for measuring ROS and oxidative stress.<sup>51</sup> It oxidizes reactive oxygen to yield fluorescent 2,7-dichlorofluorescein, resulting in an increase in fluorescence intensity.<sup>52</sup> Additional confirmation was established by employing the antioxidant NAC, which inhibited the production of ROS and significantly reduced the cell death of HeLa cells caused by HCEE treatment. These observations are a clear indication of ROS involvement in HCEE-induced apoptosis of HeLa cells.

Literature shows apoptosis to occur via extrinsic and the intrinsic pathways.<sup>53,54</sup> The binding of FasL to Fas leads to the initiation of death-inducing signal complex, eventually leading to the cleavage of caspase-8 and subsequent release of caspase-3, thus promoting apoptosis.<sup>55</sup> The results of Western blotting analysis revealed increased expression of Fas and FasL in the HeLa cells followed by activation of caspase-8.

Mitochondria too play a crucial role in activating apoptosis.<sup>56–58</sup> As evident from the DCFH-DA assay, there was a decrease in the aggregate/monomer ratio, implying mitochondrial depolarization in HeLa cells. Members of Bcl-2 family proteins control the mitochondrial apoptosis pathway by regulating mitochondrial outer membrane permeabilization.<sup>59</sup> Western blotting analysis showed that treatment of HeLa cells with HCEE increases the expression level of proapoptotic protein Bax and decreases the level of antiapoptotic protein Bcl-2. The reduced expression of Bcl-2 leads to depolarization of mitochondria membrane, resulting in mitochondrial matrix expansion by activating the caspase cascade and releasing cytochrome *c*.<sup>60</sup> The released cytochrome *c* in the presence of deoxy-ATP stimulates oligomerization of Apaf-1 into apoptosome complex and thus activates caspase cascade pathway. Caspases are a family of proteases enzymes that are broadly categorized into two functional groups: initiator caspases and executioner caspases.<sup>61</sup> Initiator caspases initiate apoptosis, while the executioner caspases play a major role in cell death machinery. Activation of procaspase-9 leads to caspase-3 activation.<sup>62</sup> Incubation of HCEE also caused increase in the expression levels of caspase-9 and caspase-3. Further, Western blotting studies showed an upregulation of cytochrome *c* and Apaf-1 in HeLa cells treated with HCEE. These findings confirmed that HCEE mediates apoptosis in HeLa cells via mitochondrial-dependent intrinsic and extrinsic apoptotic pathways (Figure 11).

Metastasis consists of a series of complicated processes involving cell migration, invasion, and adhesion.<sup>63</sup> In order to examine the antimetastasis activity of HCEE on HeLa cells, wound healing and Transwell invasion in vitro assay were performed. From the study, it was observed that HCEE restricted the invasion and migration of HeLa cells as compared to control. One of the hallmark steps that have been associated with cancer progression and metastasis in many cancer cell lines is the expression of MMP protein.<sup>64–67</sup> The MMPs are a diverse group of zinc-containing calcium-dependent endopeptidases that regulate the proteolytic cleavage of extracellular matrix proteins.<sup>68</sup> Among them, MMP-2 and MMP-9 have a major role in progression of cancer. Inhibition of MMP-9 and MMP-2 can significantly reduce tumor invasion and metastasis in cervical cancer cells.<sup>69,70</sup> In order to gain insight into the underlying mechanism of tumor invasion by HCEE, the expression of MMP-9 and MMP-2 was tested. A significant decrease in MMP-2 and MMP-9 expression levels was observed in HeLa cells exposed to HCEE as compared to untreated control. The inhibitory effect of HCEE on MMPs may be, at least in part, responsible for its antimetastatic potential.

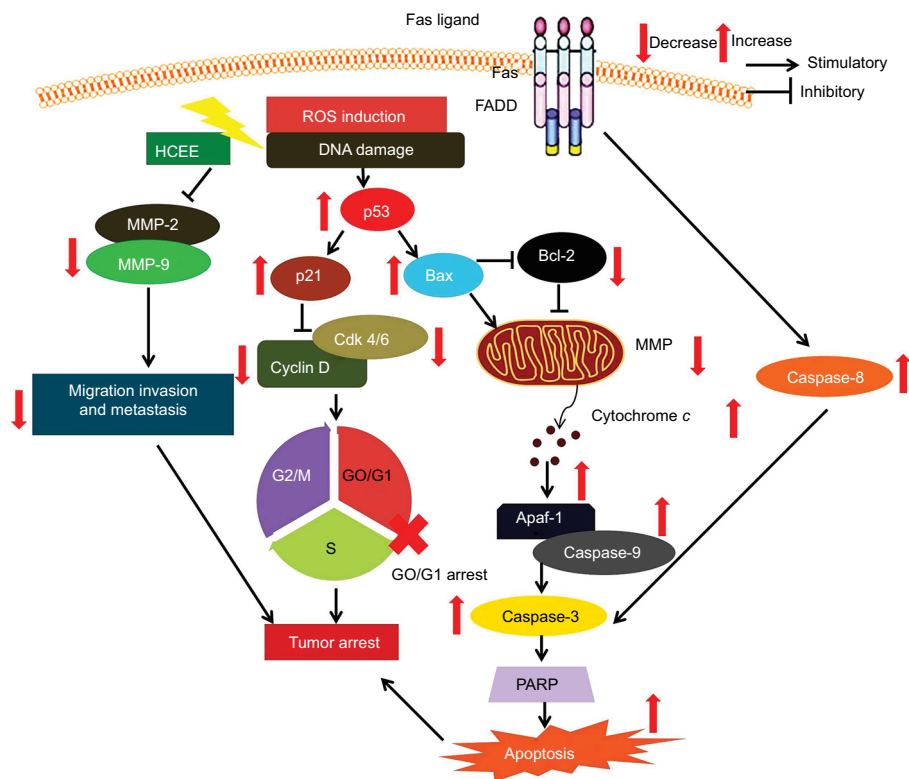


**Figure 11** Schematic representation showing the effect of HCEE on HeLa cancer cells by inducing apoptosis, promoting cell cycle arrest, and inhibiting cell migration and invasion.

**Abbreviation:** HCEE, *Hedychium coronarium* ethanol extract.

## Conclusion

The present study revealed that *H. coronarium* extract can induce apoptosis-mediated G1 phase cell arrest, while inhibiting the migratory potential of HeLa cells. G1 phase cell cycle arrest was promoted by upregulation of p53 and its effector protein p21. HCEE induced oxidative stress in HeLa cells by generating ROS and modulating the expression of antiapoptotic and proapoptotic protein levels. These processes led to depolarization of mitochondrial membrane with release of cytochrome *c*. The activation of caspase-3, caspase-8, and caspase-9 showed that the extrinsic and intrinsic pathways were involved in apoptosis. Taken together, the results of this study clearly showed that *H. coronarium* extract has clinical implications for therapeutic intervention against cervical cancer; however, further supplementary investigations in animal models are necessary to validate the anticancer activities of *H. coronarium* *in vivo*.

## Acknowledgment

The authors acknowledge the Dean, Center for Biotechnology and the Director, Regional Medical Research Center for providing necessary facilities for carrying out the research work.

## Disclosure

The authors report no conflicts of interest in this work.

## References

- Tang YQ, Jaganath IB, Sekaran SD. *Phyllanthus* spp. induces selective growth inhibition of PC-3 and MeWo human cancer cells through modulation of cell cycle and induction of apoptosis. *PLoS One*. 2010;5(9):e12644.
- Ferlay J, Soerjomataram I, Dikshit R, et al. Cancer incidence and mortality worldwide: sources, methods and major patterns in GLOBOCAN 2012. *Int J Cancer*. 2015;136(5):E359–E386.
- Narayan S, Sharma N, Kapoor A, et al. Pros and cons of adding of neoadjuvant chemotherapy to standard concurrent chemoradiotherapy in cervical cancer: a regional cancer center experience. *J Obstet Gynaecol India*. 2016;66(5):385–390.
- Wright TC Jr, Denny L, Kuhn L, Pollack A, Lorincz A. HPV DNA testing of self-collected vaginal samples compared with cytologic screening to detect cervical cancer. *JAMA*. 2000;283(1):81–86.
- Sankaranarayanan R, Budukh AM, Rajkumar R. Effective screening programmes for cervical cancer in low- and middle-income developing countries. *Bull World Health Organ*. 2001;79(10):954–962.
- Green JA, Kirwan JM, Tierney JF, et al. Survival and recurrence after concomitant chemotherapy and radiotherapy for cancer of the uterine cervix: a systematic review and meta-analysis. *Lancet*. 2001;358(9284):781–786.
- Mehta RG, Murillo G, Naithani R, Peng X. Cancer chemoprevention by natural products: how far have we come? *Pharm Res*. 2010;27(6):950–961.
- Fridlender M, Kapulnik Y, Koltai H. Plant derived substances with anti-cancer activity: from folklore to practice. *Front Plant Sci*. 2015;6:799.

9. Zhang Q, Zhang F, Thakur K, et al. Molecular mechanism of anticancerous potential of Morin extracted from mulberry in Hela cells. *Food Chem Toxicol.* 2018;112:466–475.
10. Wang J, Zhang YS, Thakur K, et al. Licochalcone A from licorice root, an inhibitor of human hepatoma cell growth via induction of cell apoptosis and cell cycle arrest. *Food Chem Toxicol.* 2018;120:407–417.
11. Seca AML, Pinto DCGA. Plant secondary metabolites as anticancer agents: successes in clinical trials and therapeutic application. *Int J Mol Sci.* 2018;19(1):E263.
12. Tang D, Kang R, Cheh CW, et al. HMGB1 release and redox regulates autophagy and apoptosis in cancer cells. *Oncogene.* 2010;29(38):5299–5310.
13. Tor YS, Yazan LS, Foo JB, et al. Induction of apoptosis in MCF-7 cells via oxidative stress generation, mitochondria-dependent and caspase-independent pathway by ethyl acetate extract of *Dillenia suffruticosa* and its chemical profile. *PLoS One.* 2015;10(6):e0127441.
14. Dai J, Mumper RJ. Plant phenolics: extraction, analysis and their anti-oxidant and anticancer properties. *Molecules.* 2010;15(10):7313–7352.
15. Ray A, Jena S, Dash B, et al. Chemical diversity, antioxidant and antimicrobial activities of the essential oils from Indian populations of *Hedychium coronarium* Koen. *Ind Crops Prod.* 2018;112:353–362.
16. Chan EW, Wong SK. Phytochemistry and pharmacology of ornamental ginger, *Hedychium coronarium* and *Alpinia purpurata*: a review. *J Integr Med.* 2015;13(6):368–379.
17. Ray A, Dash B, Sahoo A, et al. Assessment of the terpenic composition of *Hedychium coronarium* oil from Eastern India. *Ind Crops Prod.* 2017;97:49–55.
18. Shrotriya S, Ali MS, Saha A, Bachar SC, Islam MS. Anti-inflammatory and analgesic effects of *Hedychium coronarium* Koen. *Pak J Pharm Sci.* 2007;20(1):47–51.
19. Chan EWC, Lim YY, Wong LF, et al. Antioxidant and tyrosinase inhibition properties of leaves and rhizomes of ginger species. *Food Chem.* 2008;109(3):477–483.
20. Aziz MA, Habib MR, Karim MR. Antibacterial and cytotoxic activities of *Hedychium coronarium* J. Koenig. *Res J Agric Biol Sci.* 2009;5:969–972.
21. Endringer DC, Taveira FSN, Kondratyuk TP, Pezzuto JM, Braga FC. Cancer chemoprevention activity of labdane diterpenes from rhizomes of *Hedychium coronarium*. *Rev Bras Farmacogn.* 2014;24(4):408–412.
22. Chimnoi N, Pisutjaroenpong S, Ngiwsara L, et al. Labdane diterpenes from the rhizomes of *Hedychium coronarium*. *Nat Prod Res.* 2008;22(14):1249–1256.
23. Suresh G, Reddy PP, Babu KS, Shaik TB, Kalivendi SV. Two new cytotoxic labdane diterpenes from the rhizomes of *Hedychium coronarium*. *Bioorg Med Chem Lett.* 2010;20(24):7544–7548.
24. Zhan ZJ, Wen YT, Ren FY, Rao GW, Shan WG, Li CP. Diterpenoids and a diarylheptanoid from *Hedychium coronarium* with significant anti-angiogenic and cytotoxic activities. *Chem Biodivers.* 2012;9(12):2754–2760.
25. Scudiero DA, Shoemaker RH, Paull KD, et al. Evaluation of a soluble tetrazolium/formazan assay for cell growth and drug sensitivity in culture using human and other tumor cell lines. *Cancer Res.* 1988;48(17):4827–4833.
26. Purushotham G, Padma Y, Nabiha Y, Venkata Raju RR. In vitro evaluation of anti-proliferative, anti-inflammatory and pro-apoptotic activities of the methanolic extracts of *Andrographis nallamalayana* Ellis on A375 and B16F10 melanoma cell lines. *3 Biotech.* 2016;6(2):212.
27. Tian X, Guo LP, Hu XL, et al. Protective effects of *Arctium lappa* L. roots against hydrogen peroxide-induced cell injury and potential mechanisms in SH-SY5Y cells. *Cell Mol Neurobiol.* 2015;35(3):335–344.
28. Zhang Y, Chen AY, Li M, Chen C, Yao Q. *Ginkgo biloba* extract kaempferol inhibits cell proliferation and induces apoptosis in pancreatic cancer cells. *J Surg Res.* 2008;148(1):17–23.
29. Wang Y, Cheng X, Wang P, et al. Investigating migration inhibition and apoptotic effects of *Fomitopsis pinicola* chloroform extract on human colorectal cancer SW-480 cells. *PLoS One.* 2014;9(7):e101303.
30. Raza H, John A. Implications of altered glutathione metabolism in aspirin-induced oxidative stress and mitochondrial dysfunction in HepG2 cells. *PLoS One.* 2012;7(4):e36325.
31. Wang XZ, Yang HH, Li W, Han BJ, Liu YJ. Studies on apoptosis in HeLa cells via the ROS-mediated mitochondrial pathway induced by new dibenzoxanthones. *New J Chem.* 2016;40(6):5255–5267.
32. Fan C, Chen J, Wang Y, et al. Selenocystine potentiates cancer cell apoptosis induced by 5-fluorouracil by triggering reactive oxygen species-mediated DNA damage and inactivation of the ERK pathway. *Free Radic Biol Med.* 2013;65:305–316.
33. Sun W, Liu DB, Li WW, et al. Interleukin-6 promotes the migration and invasion of nasopharyngeal carcinoma cell lines and upregulates the expression of MMP-2 and MMP-9. *Int J Oncol.* 2014;44(5):1551–1560.
34. Chan EW, Wong SK. Phytochemistry and pharmacology of ornamental ginger, *Hedychium coronarium* and *Alpinia purpurata*: a review. *J Integr Med.* 2015;13(6):368–379.
35. Chen JJ, Ting CW, Wu YC, et al. New labdane-type diterpenoids and anti-inflammatory constituents from *Hedychium coronarium*. *Int J Mol Sci.* 2013;14(7):13063–13077.
36. Ebada SS, Talaat AN, Labib RM, et al. Cytotoxic labdane diterpenes and bisflavonoid atropisomers from leaves of *Araucaria bidwillii*. *Tetrahedron.* 2017;73(21):3048–3055.
37. Kunnumakkara AB, Ichikawa H, Anand P, et al. Coronarin D, a labdane diterpene, inhibits both constitutive and inducible nuclear factor- $\kappa$ B pathway activation, leading to potentiation of apoptosis, inhibition of invasion, and suppression of osteoclastogenesis. *Mol Cancer Ther.* 2008;7(10):3306–3317.
38. Chimnoi N, Sarasuk C, Khunnawutmanotham N, et al. Phytochemical reinvestigation of labdane-type diterpenes and their cytotoxicity from the rhizomes of *Hedychium coronarium*. *Phytochem Lett.* 2009;2(4):184–187.
39. Fadok VA, Bratton DL, Rose DM, Pearson A, Ezekewitz RA, Henson PM. A receptor for phosphatidylserine-specific clearance of apoptotic cells. *Nature.* 2000;405(6782):85–90.
40. Huynh ML, Fadok VA, Henson PM. Phosphatidylserine-dependent ingestion of apoptotic cells promotes TGF- $\beta$ 1 secretion and the resolution of inflammation. *J Clin Invest.* 2002;109(1):41–50.
41. Pucci B, Kasten M, Giordano A. Cell cycle and apoptosis. *Neoplasia.* 2000;2(4):291–299.
42. Pietenpol JA, Stewart ZA. Cell cycle checkpoint signaling: cell cycle arrest versus apoptosis. *Toxicology.* 2002;181–182:475–481.
43. Evan GI, Vousden KH. Proliferation, cell cycle and apoptosis in cancer. *Nature.* 2001;411(6835):342–348.
44. Murray AW. Recycling the cell cycle: cyclins revisited. *Cell.* 2004;116(2):221–234.
45. Looi CY, Arya A, Cheah FK, et al. Induction of apoptosis in human breast cancer cells via caspase pathway by vernodalin isolated from *Centratherum anthelminticum* (L.) seeds. *PLoS One.* 2013;8(2):e56643.
46. Malumbres M. Cyclin-dependent kinases. *Genome Biol.* 2014;15(6):122.
47. Malumbres M, Barbacid M. Milestones in cell division: to cycle or not to cycle: a critical decision in cancer. *Nat Rev Cancer.* 2001;1:222.
48. Lee J, Giordano S, Zhang J. Autophagy, mitochondria and oxidative stress: cross-talk and redox signalling. *Biochem J.* 2012;441(2):523–540.
49. Scherz-Shouval R, Elazar Z. Regulation of autophagy by ROS: physiology and pathology. *Trends Biochem Sci.* 2011;36(1):30–38.
50. Lebel CP, Ischiropoulos H, Bondy SC. Evaluation of the probe 2',7'-dichlorofluorescein as an indicator of reactive oxygen species formation and oxidative stress. *Chem Res Toxicol.* 1992;5(2):227–231.
51. Gomes A, Fernandes E, Lima JL. Fluorescence probes used for detection of reactive oxygen species. *J Biochem Biophys Methods.* 2005;65(2–3):45–80.
52. Xu G, Shi Y. Apoptosis signaling pathways and lymphocyte homeostasis. *Cell Res.* 2007;17(9):759–771.

53. Ko YC, Lien JC, Liu HC, et al. Demethoxycurcumin induces the apoptosis of human lung cancer NCI-H460 cells through the mitochondrial-dependent pathway. *Oncol Rep.* 2015;33(5):2429–2437.
54. Kim HJ, Yang KM, Park YS, et al. The novel resveratrol analogue HS-1793 induces apoptosis via the mitochondrial pathway in murine breast cancer cells. *Int J Oncol.* 2012;41(5):1628–1634.
55. Desagher S, Martinou JC. Mitochondria as the central control point of apoptosis. *Trends Cell Biol.* 2000;10(9):369–377.
56. Wang X. The expanding role of mitochondria in apoptosis. *Genes Dev.* 2001;15(22):2922–2933.
57. Kim JS, He L, Lemasters JJ. Mitochondrial permeability transition: a common pathway to necrosis and apoptosis. *Biochem Biophys Res Commun.* 2003;304(3):463–470.
58. Danial NN, Korsmeyer SJ. Cell death: critical control points. *Cell.* 2004;116(2):205–219.
59. Brunelle JK, Letai A. Control of mitochondrial apoptosis by the Bcl-2 family. *J Cell Sci.* 2009;122(Pt 4):437–441.
60. Saleh A, Srinivasula SM, Acharya S, Fishel R, Alnemri ES. Cytochrome *c* and dATP-mediated oligomerization of Apaf-1 is a prerequisite for procaspase-9 activation. *J Biol Chem.* 1999;274(25):17941–17945.
61. Kumar S. Regulation of caspase activation in apoptosis: implications in pathogenesis and treatment of disease. *Clin Exp Pharmacol Physiol.* 1999;26(4):295–303.
62. Brentnall M, Rodriguez-Menocal L, De Guevara RL, Cepero E, Boise LH. Caspase-9, caspase-3 and caspase-7 have distinct roles during intrinsic apoptosis. *BMC Cell Biol.* 2013;14(1):32.
63. Chen J, Thompson LU. Lignans and tamoxifen, alone or in combination, reduce human breast cancer cell adhesion, invasion and migration in vitro. *Breast Cancer Res Treat.* 2003;80(2):163–170.
64. Fan MJ, Wang IC, Hsiao YT, et al. Anthocyanins from black rice (*Oryza sativa* L.) demonstrate antimetastatic properties by reducing MMPs and NF- $\kappa$ B expressions in human oral cancer CAL 27 cells. *Nutr Cancer.* 2015;67(2):327–338.
65. Tsai JR, Liu PL, Chen YH, et al. Curcumin inhibits non-small cell lung cancer cells metastasis through the adiponectin/NF- $\kappa$ B/MMPs signaling pathway. *PLoS One.* 2015;10(12):e0144462.
66. Xia Y, Lian S, Khoi PN, et al. Chrysin inhibits tumor promoter-induced MMP-9 expression by blocking AP-1 via suppression of ERK and JNK pathways in gastric cancer cells. *PLoS One.* 2015;10(4):e0124007.
67. Yan H, Xin S, Wang H, Ma J, Zhang H, Wei H. Baicalein inhibits MMP-2 expression in human ovarian cancer cells by suppressing the p38 MAPK-dependent NF- $\kappa$ B signaling pathway. *Anticancer Drugs.* 2015;26(6):649–656.
68. Jabłońska-Trypuć A, Matejczyk M, Rosochacki S. Matrix metalloproteinases (MMPs), the main extracellular matrix (ECM) enzymes in collagen degradation, as a target for anticancer drugs. *J Enzyme Inhib Med Chem.* 2016;31(sup1):177–183.
69. Chu SC, Yu CC, Hsu LS, Chen KS, Su MY, Chen PN. Berberine reverses epithelial-to-mesenchymal transition and inhibits metastasis and tumor-induced angiogenesis in human cervical cancer cells. *Mol Pharmacol.* 2014;86(6):609–623.
70. Koppikar SJ, Choudhari AS, Suryavanshi SA, Kumari S, Chattopadhyay S, Kaul-Ghanekar R. Aqueous cinnamon extract (ACE-c) from the bark of *Cinnamomum cassia* causes apoptosis in human cervical cancer cell line (SiHa) through loss of mitochondrial membrane potential. *BMC Cancer.* 2010;10(1):210.

## Cancer Management and Research

### Publish your work in this journal

Cancer Management and Research is an international, peer-reviewed open access journal focusing on cancer research and the optimal use of preventative and integrated treatment interventions to achieve improved outcomes, enhanced survival and quality of life for the cancer patient. The manuscript management system is completely online and includes

a very quick and fair peer-review system, which is all easy to use. Visit <http://www.dovepress.com/testimonials.php> to read real quotes from published authors.

Submit your manuscript here: <https://www.dovepress.com/cancer-management-and-research-journal>

Dovepress